

Optimization of modular Truss-Z by minimum-mass design under equivalent stress constraint

Machi Zawidzki^{*}, Łukasz Jankowski^a

*Institute of Fundamental Technological Research, Polish Academy of Sciences,
ul. Pawińskiego 5B, 02-106 Warsaw, Poland*

(Received keep as blank , Revised keep as blank , Accepted keep as blank)

Abstract. Truss-Z (TZ) is an Extremely Modular System (EMS). Such systems allow for creation of structurally sound free-form structures, are comprised of as few types of modules as possible, and are not constrained by a regular tessellation of space. Their objective is to create spatial structures in given environments connecting given terminals without self-intersections and obstacle-intersections. TZ is a skeletal modular system for creating free-form pedestrian ramps and ramp networks. The previous research on TZ focused on global discrete geometric optimization of the spatial configuration of modules. This paper reports on the first attempts at structural optimization of the module for a single-branch TZ. The internal topology and the sizing of module beams are subject to optimization. An important challenge is that the module is to be *universal*: it must be designed for the worst case scenario, as defined by the module position within a TZ branch and the geometric configuration of the branch itself. There are four variations of each module, and the number of unique TZ configurations grows exponentially with the branch length. The aim is to obtain minimum-mass modules with the von Mises equivalent stress constrained under certain design load. The resulting modules are further evaluated also in terms of the typical structural criterion of compliance.

Keywords: Extremely Modular System; Truss-Z; structural optimization; modular structures; minimum mass design; frame structures

1. Introduction

A stairway is the most common means of pedestrian vertical transportation used in the built environment. Elevators and escalators are relatively expensive to install and maintain, and their traffic flow capacity is much lower than that of stairs. Moreover, it is not always possible to install an elevator or escalator due to limited space. However, most people occasionally or temporarily cannot use stairs, as when riding a bicycle, pushing a baby stroller or carrying heavy luggage. For elders and people in wheelchairs, stairs form a permanent and impassable barrier. This is an important social issue, especially since the proportion of elderly people in society is higher than in the past, and some predict that this tendency will continue (Pollack 2005). A comprehensive literature review for elderly pedestrians is carried out in Dunbar *et al.* (2004).

^{*}Corresponding author, Assist. Prof., E-mail: zawidzki@mit.edu

^a Assoc. Prof., E-mail: ljank@ippt.pan.pl

Truss-Z (TZ) is an Extremely Modular System (EMS). In such systems, the assembly, reconfiguration and deployment difficulty is moved towards the module, which is relatively complex and whose assembly is not intuitive. As a result, an EMS requires intensive computation for assembling its desired free-form geometrical configuration, while its advantage is the economization of construction and reconfiguration by extreme modularization and mass prefabrication. TZ is a modular skeletal system for creating free-form ramps and ramp networks among any number of terminals in space. The concept has been introduced in Zawidzki and Tateyama (2011). The motivation for TZ in the context of human mobility, and in particular the mobility problems of elders is discussed in Zawidzki (2015). The underlying idea of this system is to create structurally sound provisional or permanent structures using the minimal number of types of modular elements. Further discussion on modularity vs. free-form can be found in Zawidzki (2015).

TZ is comprised of Truss-Z modules, TZMs for short. In principle, a single-branch TZ connects two points in space, called terminals. Constructing an efficient TZ can be formally expressed as a constrained discrete multicriterial optimization problem. In the previous research only the geometrical properties, such as the total number of modules (n), “geometrical simplicity” (G_S) and “number of turns” (N_T), have been minimized. The criteria G_S and N_T measure how many units do not follow a straight line, and how many continuous turns there are in the path, respectively. Common constraints have been the locations of terminals, positions and shapes of obstacles in the environment, etc. This paper focuses on structural performance of the resulting TZs and reports on the first attempt at structural optimization of a TZM for a single-branch TZ. Research on structural optimization of modular structures seems to be relatively sparse. Tugilimana *et al.* (2017) consider layout optimization of a modular bridge, where the design variables are effectively discrete and encode the choice from a predefined set of local module topologies. Simultaneous optimization of a family of a few vehicle structures at the level of the shared basic beam components is discussed in Torstenfelt and Klarbring (2006). Here, the main difference with respect to typical structural optimization problems (Christensen and Klarbring 2009) is linked to the modularity of the TZ: the optimization is performed at the level of a single module, each module can however occur (i) in four different variations, (ii) at a different position within the TZ branch, and (iii) the TZ itself can assume a large number of different geometrical configurations. Therefore, instead of a typical single structure and a predefined single/multiple load conditions, all the related structural configurations need to be simultaneously assessed in order to optimize their worst-case performance. The following assumptions have been made:

1. The TZ is modeled as a 3D frame structure.
2. The beams are modeled using the finite element (FE) method as Euler-Bernoulli beams with the properties of circular hollow sections.
3. The maximum span of TZ is seven modules (i.e., the branches are supported at least every seventh module).
4. The outer shape of the module is fixed.
5. The maximum von Mises equivalent stress under certain static design load is constrained from above.

Subject to minimization is the total mass of TZM. The sizing of the TZM beams is defined by their diameters, which are treated as the optimization variables. To account for various internal topologies of the module, the minimization is performed separately for each of 16 possible orientations of the diagonal beams and for various TZ lengths. Finally, the optimized modules are assessed in terms of the achieved minimum mass and the compliance, which is a typical aggregate

measure of structural stiffness.

The paper is structured as follows. Section 2 briefly introduces the concept and the motivation for the modular Truss-Z system. The geometry and topology of a single module is presented in Section 3. Section 4 discusses the optimization process, including the optimization variables, the static load scheme and the constraints. The optimization results are presented and discussed in Section 5.

2. Truss-Z modular system

2.1 The concept

In geometrical terms, all TZ structures are composed of only four variations (affine transformations) of a single basic unit or module (R). Fig. 1 shows the geometrical properties of R which have been set arbitrarily based on functional criteria and used in theretofore research. Unit L is a mirror reflection of the unit R . By rotation, they can be assembled in two additional ways (R_2 is the rotated R , and L_2 is the rotated L), effectively giving four types of units. Some examples are shown in Fig. 2. Fig. 3 shows a visualization of retrofitting of an existing site with a TZ system.

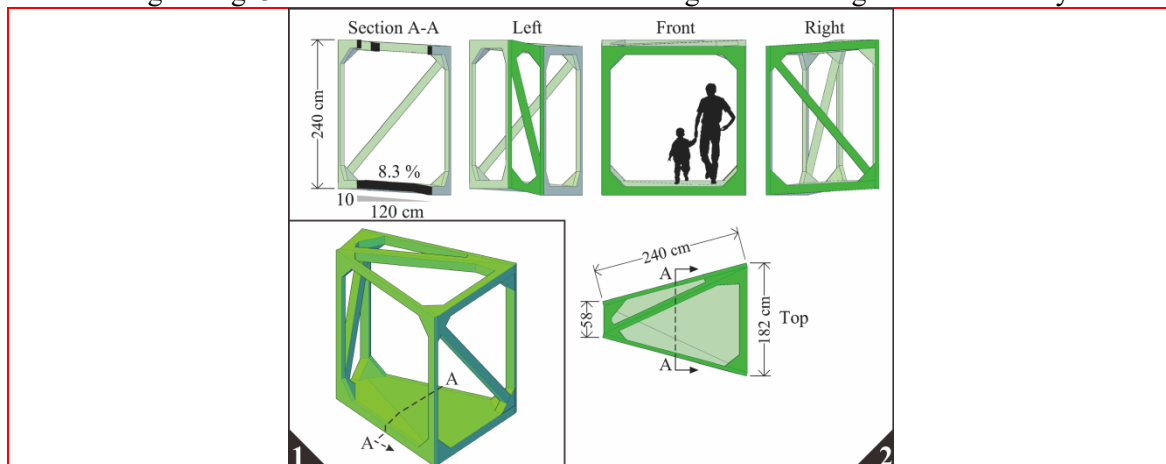
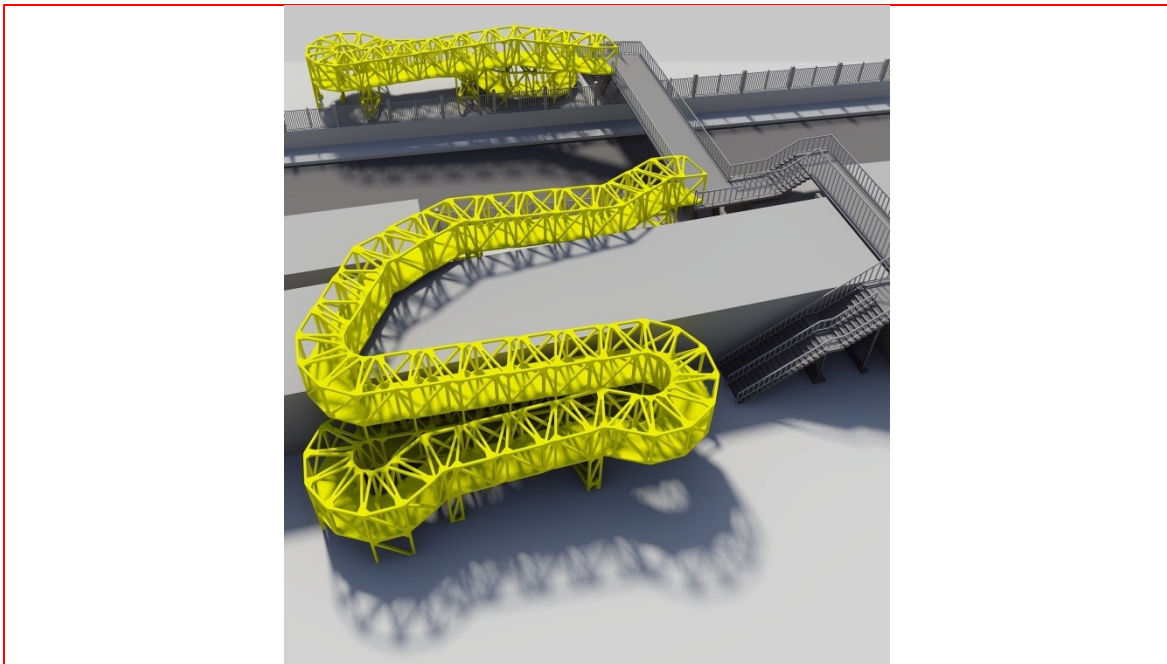
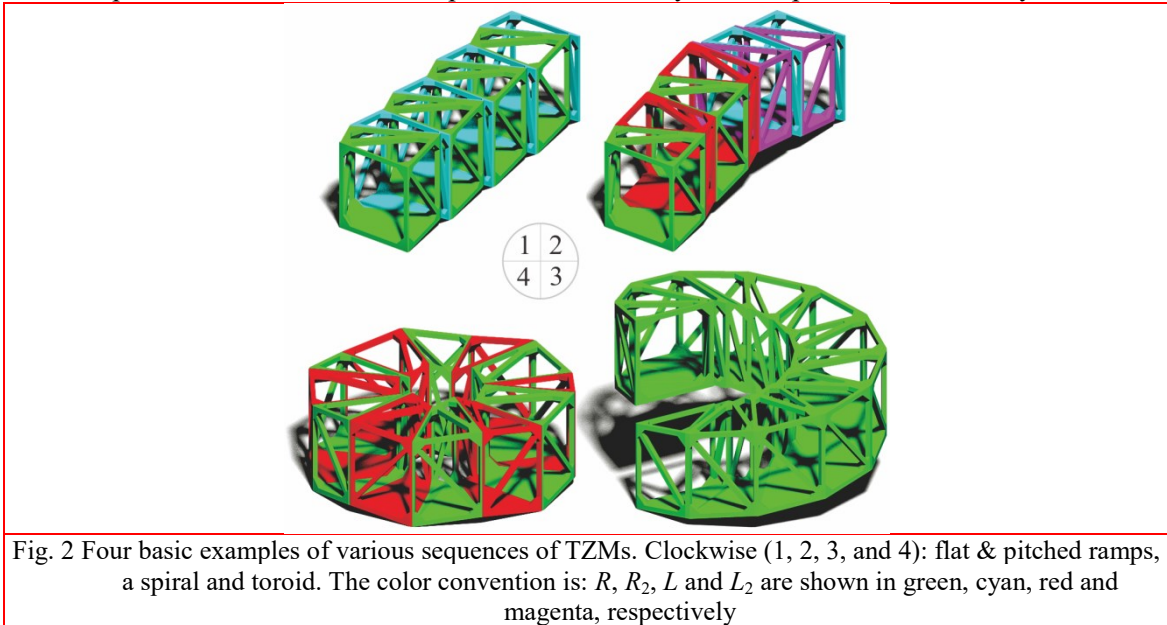


Fig. 1 (1) Axonometric view of the original TZ basic unit R . (2) From the left: section A–A showing the slope, and four orthographic views

Due to the modularity of this system, it is natural to apply discrete optimization methods for creating TZ connectors and networks. In geometrical terms, such structures can be optimized for various criteria: the minimal number of modules, the minimal number of changes in direction, and in a case of multiple branches, the minimal network distance, etc. Various deterministic and meta-heuristic methods have been successfully implemented for single-branch TZ paths, including backtracking (Zawidzki 2011), evolution strategy (Zawidzki and Tateyama 2011), and evolutionary algorithms (Zawidzki and Nishinari 2013). These methods produced usually good, but not ideal, solutions. A graph-theoretical exhaustive search method, which produces the best allowable, that is ideal solutions, has been described in Zawidzki (2013). Even though the structural rigidity of the TZ module has been demonstrated in Zawidzki and Nishinari (2012), along with other topology-related properties such as nullity and the degree of static indeterminacy,

there is up to now no consistent attempt at structural analysis and optimization of the system.



2.2 Truss-Z module geometry

The geometry of the module is determined by five parameters: planar angle θ , width r , “slenderness” s , vertical displacement δ_z , and height h , as shown in Fig. 4. The slenderness s is the ratio between the offset from the apex d to the width r . For the three cases of $s = 0$, $0 < s < \infty$ and $s = \infty$, the corresponding projections of TZM form a triangle, a trapezoid, and a rectangle, respectively.

The outer shape of TZM, as presented in theretofore investigations, is based on functional considerations and remains unaltered in this paper. It is defined by the following parameter values: $\theta = 30^\circ$, $r = 2.4$ m, $s = 0.5$, $\delta_z = 0.1$ m, and $h = 2.4$ m.

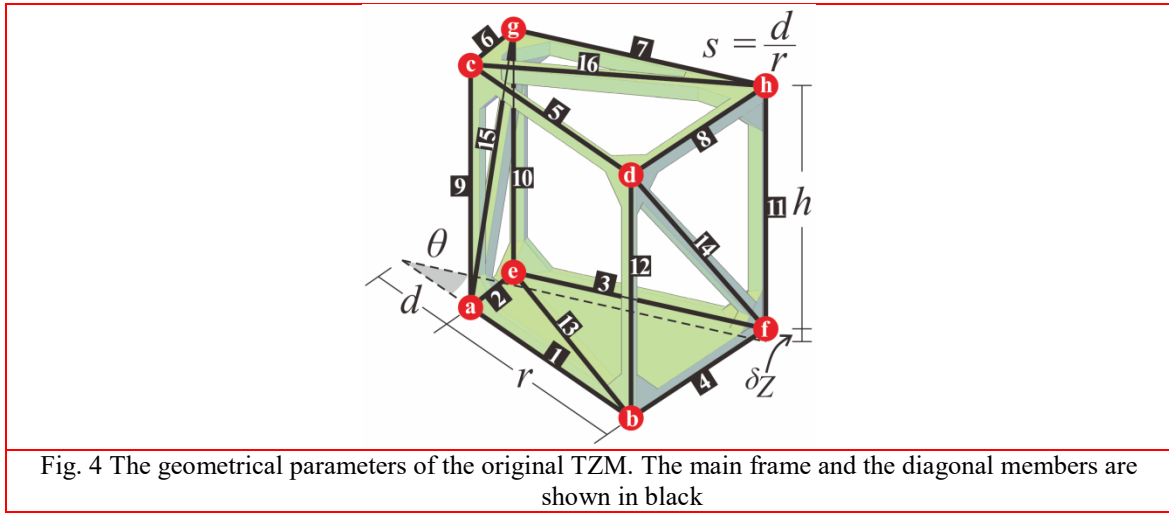


Fig. 4 The geometrical parameters of the original TZM. The main frame and the diagonal members are shown in black

3. Structural optimization of a TZM

3.1 Optimization variables

The outer geometry of a Truss-Z module has been proven in earlier research to be functional and flexible enough to create free-form shaped ramps in complex environments. Thus, the geometry of the main frame of a module is treated here as fixed, and the structural optimization process is limited to two factors:

- *Diameters of the beams* (\mathbf{x}). Each TZM is modeled as a 3D frame and consists of 16 beams. The material parameters are assumed to correspond to steel with the density of 7850 kg/m^3 , Young's modulus 210 GPa , and the shear modulus of 81 GPa . For optimization purposes, it is assumed that each beam is a circular hollow section with the width of the wall equal to 2 mm , and that only the outer diameters of the sections are subject to sizing optimization. The corresponding 16-element vector is denoted by \mathbf{x} ,

$$\mathbf{x} = (\varphi_1, \varphi_2, \dots, \varphi_{16}). \quad (1)$$

The successive components of the vector \mathbf{x} correspond to the TZM beams as marked in Fig. 4.

- *Placement of the diagonal beams (d)*. There are four module faces with a diagonal beam (floor, ceiling and two sides) and each diagonal can assume two configurations, there is thus a total of $2^4 = 16$ different possible configurations of the diagonal beams. They are denoted by a sequence d of four binary digits (or alternatively, the corresponding decimal number) that describe respectively the configuration of the diagonal within the floor, the longer side wall, the shorter side wall, and the ceiling. The digits of d correspond to the components φ_{13} to φ_{16} of the vector \mathbf{x} (beams No. 13 to 16 in Fig. 4). For example, the specific configuration shown in Fig. 4 is denoted by the binary sequence $d = 0000_2$, that is the decimal number 0. The general encoding scheme is presented in Table 1.

Notice that in different configurations the two side diagonals have different lengths (2.960 m vs. 3.118 m and 2.576 m vs. 2.382 m), which suggests that the structural effects of configuration might be related not only to purely topological differences, but also to the lengths and masses of the side diagonal beams.

Table 1 Encoding scheme d for the diagonal beams. TZM beams and nodes are numbered as in Fig. 4

beam No	13		14		15		16	
end nodes	be	af	df	bh	ag	ce	ch	dg
digits of d	0	1	0	1	0	1	0	1
$d=0$	0		0		0		0	
$d=1$	0		0		0		1	
$d=2$	0		0		1		0	
$d=3$	0		0		1		1	
$d=4$	0		1		0		0	
$d=5$	0		1		0		1	
$d=6$	0		1		1		0	
$d=7$	0		1		1		1	
$d=8$	1		0		0		0	
$d=9$	1		0		0		1	
$d=10$	1		0		1		0	
$d=11$	1		0		1		1	
$d=12$	1		1		0		0	
$d=13$	1		1		0		1	
$d=14$	1		1		1		0	
$d=15$	1		1		1		1	

3.2 Constraints

The structural safety of a TZ structure constructed using modules of beam diameters \mathbf{x} and with diagonal configuration d is quantified here in terms of the maximum value of the von Mises equivalent stress $\sigma^{\text{eq}}(\mathbf{x}, d, s)$ that occurs in the (entire) TZ structure under the assumed static load

vector $\mathbf{F}(d, s)$, see Section 3.3. The symbol s denotes a specific geometric configuration of the modules that uniquely determines the entire Truss-Z (for example configurations see Fig. 2).

The TZ system has a modular character, so that the ultimate configuration s used in a specific environment is not known in advance. As a result, one needs to assess structurally not a single specific configuration s of the modules, but rather the worst case of a certain set S of configurations that are expected to be used in real environments (Calafiore and Dabene 2008). The set S considered here is one of the six following sets,

$$S \in \{S_2, S_3, \dots, S_7\}. \quad (2)$$

In Eq. (2), S_n denotes the set of all TZ structures of length n with fixed supports in all degrees of freedom of the entrance and exit square plane frames: set S_2 is the set of all 2-element TZs, set S_3 is the set of all 3-element TZs, etc. The choice of the particular value of n in practice will be based on practical considerations, since it amounts to the assumption that the TZ ramp is supported not sparser than every n modules. As each module occurs in four variations (R, L, R_2, L_2), the total number of configurations in S_n is in general 4^n . However, this number can be decreased by considering only essentially unique configurations, that is configurations unique up to the left–right and entrance–exit structural symmetries, as well as to their superposition (rotation). For example, the number of essentially unique 2-module TZs is 6 instead of 16 ($RR, RR_2, RL, RL_2, L_2R, L_2L$). In general, it can be shown that the total number \bar{S}_n of essentially unique n -module configurations is

$$\bar{S}_n = \begin{cases} 4^{n-1} & \text{if } n \text{ is odd,} \\ 4^{n-1} + 2^{n-1} & \text{if } n \text{ is even} \end{cases} \quad (3)$$

or 6, 16, 72, 256, 1056 and 4096 respectively for $n = 2, 3, \dots, 7$. The sets S_2 and S_4 are depicted in Fig. 5 and Fig. 6 using the same color convention as in Fig. 2. The safety criterion for a TZ module is thus defined based on the worst-case among all S_n possible scenarios: it is the maximum equivalent stress of the beams in all modules in all possible configurations $s \in S_n$ subjected to the assumed static load $\mathbf{F}(d, s)$,

$$\sigma^{\text{eq}}(\mathbf{x}, d, S_n) := \max_{s \in S_n} \sigma^{\text{eq}}(\mathbf{x}, d, s). \quad (4)$$

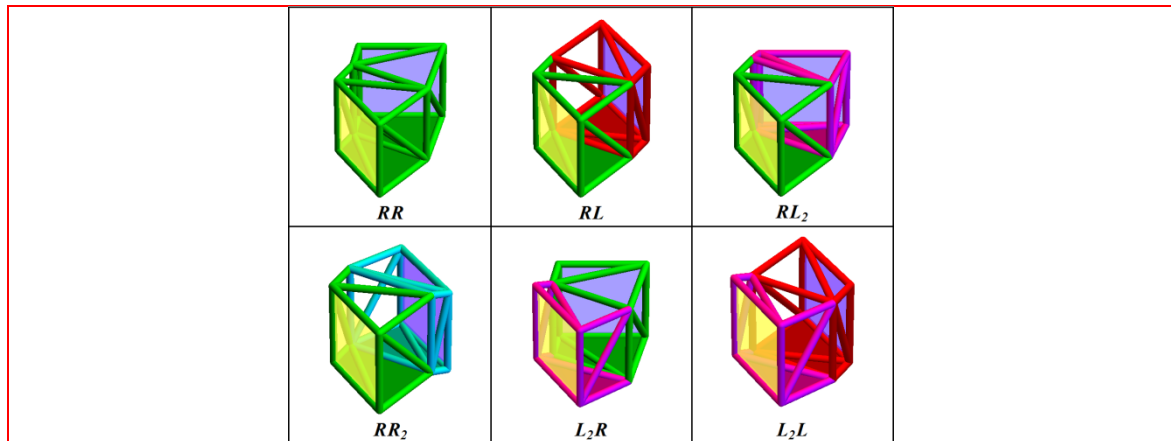


Fig. 5 The set S_2 of all essentially unique TZ structures of length 2. Module color convention as in Fig. 2. The fixing planes at the first and last module are indicated in: yellow and blue, respectively





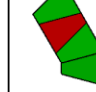











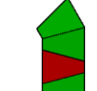
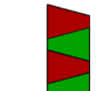




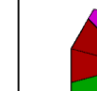
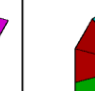
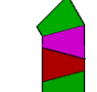
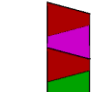




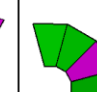
















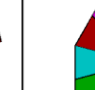
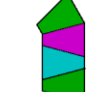



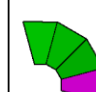
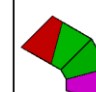










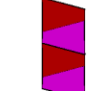




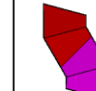


 <i>RRRR</i>	 <i>RRRL</i>	 <i>RRRL₂</i>	 <i>RRRR₂</i>	 <i>RRLR</i>	 <i>RRLL</i>	 <i>RRLL₂</i>	 <i>RRLR₂</i>
 <i>RRL₂R</i>	 <i>RRL₂L</i>	 <i>RRL₂L₂</i>	 <i>RRL₂R₂</i>	 <i>RRR₂R</i>	 <i>RRR₂L</i>	 <i>RRR₂L₂</i>	 <i>RRR₂R₂</i>
 <i>RLRR</i>	 <i>RLRL</i>	 <i>RLRL₂</i>	 <i>RLRR₂</i>	 <i>RLLR</i>	 <i>RLLL</i>	 <i>RLLL₂</i>	 <i>RLLR₂</i>
 <i>RLL₂R</i>	 <i>RLL₂L</i>	 <i>RLL₂R₂</i>	 <i>RLR₂R</i>	 <i>RLR₂L</i>	 <i>RLR₂L₂</i>	 <i>RL₂RR</i>	 <i>RL₂RL</i>
 <i>RL₂RL₂</i>	 <i>RL₂RR₂</i>	 <i>RL₂LR</i>	 <i>RL₂LL</i>	 <i>RL₂LL₂</i>	 <i>RL₂LR₂</i>	 <i>RL₂L₂R</i>	 <i>RL₂L₂L</i>
 <i>RL₂R₂R</i>	 <i>RL₂R₂L</i>	 <i>RR₂RR</i>	 <i>RR₂RL</i>	 <i>RR₂RR₂</i>	 <i>RR₂LR</i>	 <i>RR₂LL</i>	 <i>RR₂LL₂</i>
 <i>RR₂L₂R</i>	 <i>RR₂L₂L</i>	 <i>RR₂R₂R</i>	 <i>RR₂R₂L</i>	 <i>L₂RRR</i>	 <i>L₂RRL</i>	 <i>L₂RLR</i>	 <i>L₂RLL</i>
 <i>L₂RL₂R</i>	 <i>L₂RL₂L</i>	 <i>L₂RR₂R</i>	 <i>L₂RR₂L</i>	 <i>L₂LRR</i>	 <i>L₂LRL</i>	 <i>L₂LLR</i>	 <i>L₂LLL</i>
 <i>L₂LL₂L</i>	 <i>L₂LR₂R</i>	 <i>L₂L₂RR</i>	 <i>L₂L₂RL</i>	 <i>L₂L₂LR</i>	 <i>L₂L₂LL</i>	 <i>L₂R₂RL</i>	 <i>L₂R₂LR</i>

Fig. 6 The set S_4 of all essentially unique TZ structures of length 4. Module color convention as in Fig. 2

Consequently, the optimization variables $\mathbf{x} = (\varphi_1, \varphi_2, \dots, \varphi_{16})$ and d are constrained as follows:

- To ensure the safety of the structure, the von Mises equivalent stress in the entire structure is required to be below 100 MPa, which is a value assumed safe for steel,

$$\sigma^{\text{eq}}(\mathbf{x}, d, S_n) \leq 100 \text{ MPa.} \quad (5)$$

- Since each section wall is 2 mm thick, there is an obvious lower bound constraint on the section diameters,

$$\varphi_i \geq 4 \text{ mm.} \quad (6)$$

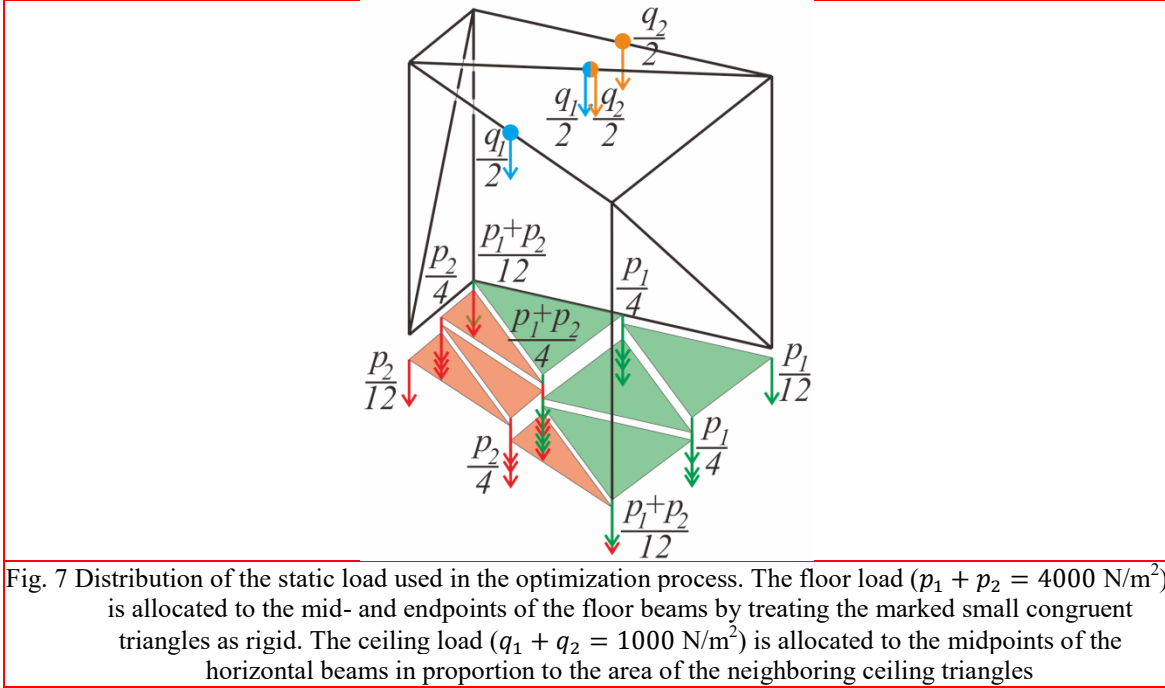
- The placement d of the diagonal beams is a 4-digit binary number, thus

$$0 \leq d \leq 15, \quad d \in \mathbb{N}. \quad (7)$$

In numerical computations, the 3D Euler–Bernoulli beam finite elements are employed to obtain the element forces, which are then used with the circular hollow section formulas to yield the maximum equivalent von Mises stress of each section.

3.3 Static load scheme

The optimization is performed in the static case, in which the entire Truss-Z structure is subjected to a certain static load $\mathbf{F}(d, s)$. The load is assumed to correspond to the static vertical load of 5000 N/m^2 , which is distributed in proportion 4:1 between the ceiling and floor levels, and then allocated to the end- and midpoints of the respective horizontal beams proportionally to the area of the neighboring triangles. Load distribution for a single module is shown in Fig. 7, where p_1, p_2 and q_1, q_2 denote the area loads per two triangles of the floor and the ceiling, respectively. For load allocation purposes, each of the two floor triangles is further divided into four congruent triangles that are treated as rigid. It allows their area loads ($p_1/4$ and $p_2/4$) to be distributed evenly to their vertices. Given a TZ structure $s \in S_n$, each of its modules is subjected separately to such a load, which are then all assembled into the global load $\mathbf{F}(d, s)$ of the entire structure.



3.4 Assessment criteria

The aim of the optimization is to minimize the total mass $m(\mathbf{x}, d)$ of the module with respect to beam diameters \mathbf{x} , subject to the constraints stated in Section 3.2, in dependence on the configuration d of the diagonal beams. Due to the discrete nature of the variable d , see Eq. (7), the optimization is performed separately for each of the 16 diagonal configurations, $d \in \{0, 1, \dots, 15\}$, and then repeated for each considered length of the TZ branch, $S \in \{S_2, S_3, \dots, S_7\}$. The resulting mass-minimum designs,

$$\begin{aligned} \bar{\mathbf{x}}(d, S_n) &:= \arg \min_{\mathbf{x}} m(\mathbf{x}, d) \\ &\text{s.t. Eqs. (5)-(6),} \end{aligned} \quad (8)$$

are assessed in terms of the following two structural criteria:

- *Module mass*, that is the achieved minimum value of the objective function,

$$\bar{m}(d, S_n) := \bar{m}(\bar{\mathbf{x}}(d, S_n), d). \quad (9)$$

- The *worst-case compliance* under the assumed static load. The compliance, a typical measure of structural stiffness (Christensen and Klarbring 2009), is computed for all the configurations $s \in S_n$, and then the maximum value is selected to represent the worst case,

$$\bar{C}(d, S_n) := \max_{s \in S_n} [\mathbf{F}(d, s)]^T \mathbf{u}(\bar{\mathbf{x}}(d, S_n), s, \mathbf{F}(d, s)), \quad (10)$$

where $\mathbf{u}(\mathbf{x}, s, \mathbf{F})$ is the displacement vector for the TZ composed of modules with beam diameters \mathbf{x} in configuration s and subjected to the static load \mathbf{F} .

The entire optimization procedure is outlined in Appendix in Table 3

4. Optimization results

4.1 Configuration of diagonals

Minimization of the module mass Eq. (8) has been performed separately for each diagonal configuration d and for each considered branch length $n \in \{2, 3, \dots, 7\}$. All the results are shown together in Fig. 8. The horizontal axis represents the achieved minimum mass Eq. 9, while the vertical axis represents the worst-case (maximum) compliance of the corresponding mass-minimum TZ structures of length n , as defined in Eq. 10. Each point corresponds to a specific pair of parameters (n, d) . The points form clearly distinguishable clusters of 16 points. The clusters correspond to the different considered branch lengths $n = 2, 3, \dots, 7$ that are accordingly labeled in the figure and recognizable by the increasingly larger masses of the optimum modules. Larger and optimally distributed mass means a stiffer module, so that for longer TZs the worst-case compliance decreases with the increasing length of the TZ branch, even though the branch bears a larger total design load.

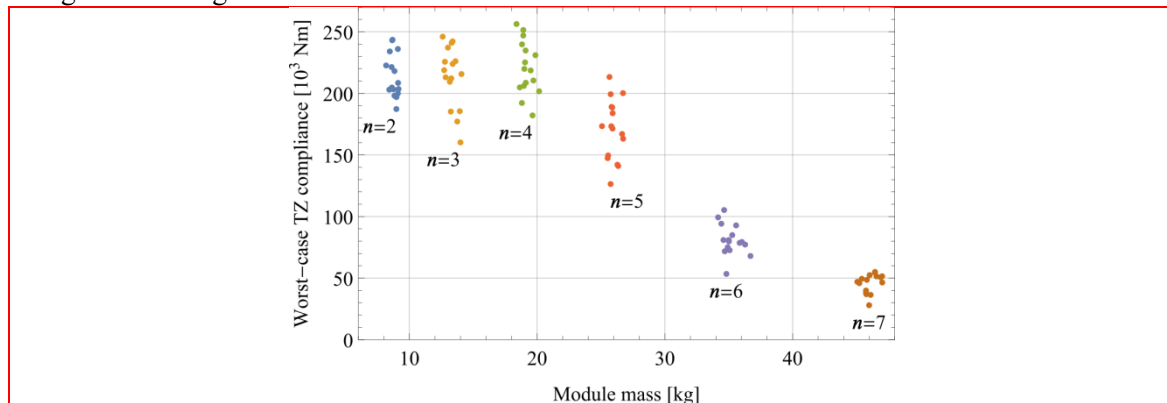


Fig. 8 Results of the optimization, shown in the space of the achieved minimum module mass vs. the worst-case compliance of the entire TZ. Point clusters correspond to the TZ branches of the lengths $n = 2$ to $n = 7$. Points within each cluster correspond to the 16 possible configurations d of the diagonal beams in the specific optimized mass-minimum module

Within a cluster, each point corresponds to a specific configuration d of the diagonal beams in the optimized mass-minimum module. The detailed views for separate clusters are shown magnified in Figs. 9-14. The optimum point within each cluster (that is the optimum configuration of the diagonal beams d) can be found by weighing the achieved minimum mass of the module vs. the worst-case (maximum) compliance of the corresponding TZ, which amounts to selecting a point on the Pareto front of each cluster. The diagonal configurations d that form the Pareto fronts for each cluster are marked in the plots and listed in Table 2 in the order of the increasing module mass (decreasing worst-case compliance). It can be noticed that the only diagonal configurations present in the Pareto fronts of all clusters are $d = 2$ and $d = 9$, and that for all but

the shortest TZ branch the configuration $d = 2$ is the ultimate mass-minimum. These two configurations, see Fig. 15, can be thus considered as universally optimal, irrespective of the length of the specific TZ branch in-between the successive structural supports.

Due to the relatively small size of the discrete design space (16 diagonal configurations x 6 branch lengths), it is possible here to explore it entirely. However, problems with a more complex and a larger design space would require an application of a heuristic optimization algorithm.

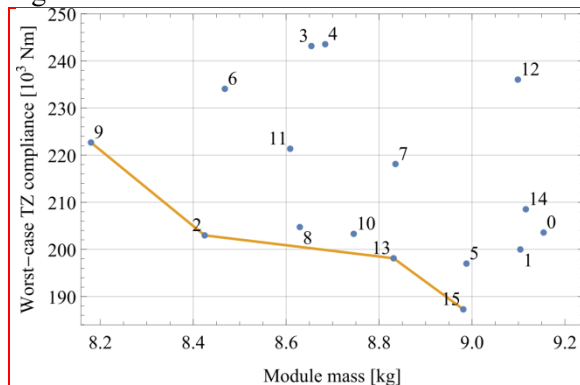


Fig. 9 The point cluster corresponding to the TZ branch of length $n=2$ with marked Pareto front

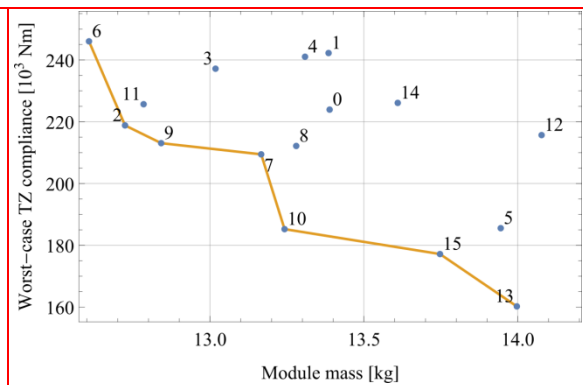


Fig. 10 The point cluster corresponding to the TZ branch of length $n=3$ with marked Pareto front

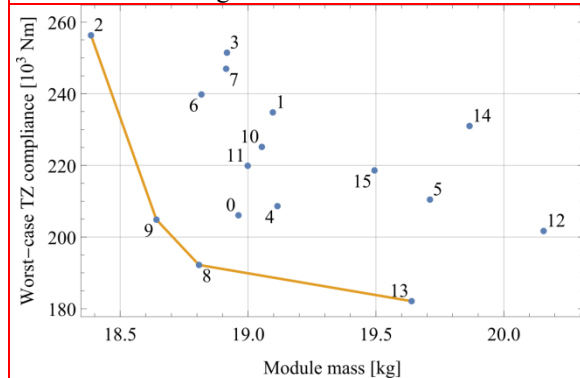


Fig. 11 The point cluster corresponding to the TZ branch of length $n=4$ with marked Pareto front

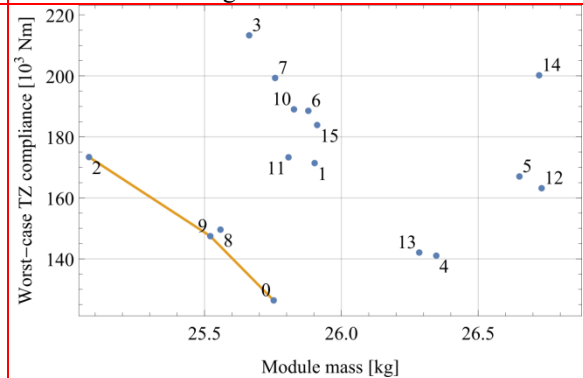


Fig. 12 The point cluster corresponding to the TZ branch of length $n=5$ with marked Pareto front

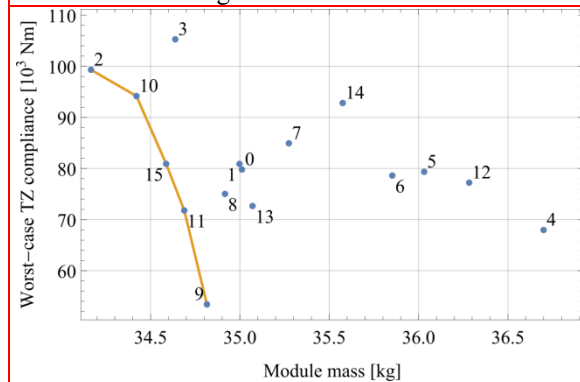


Fig. 13 The point cluster corresponding to the TZ branch of length $n=6$ with marked Pareto front

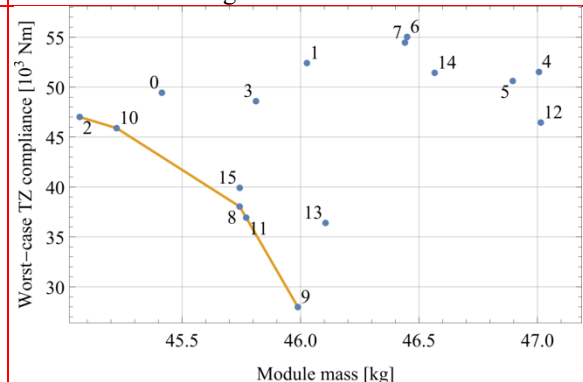


Fig. 14 The point cluster corresponding to the TZ branch of length $n=7$ with marked Pareto front

Table 2 The diagonal configurations d from the Pareto front for each considered TZ branch length n , listed in the order of increasing module mass and decreasing worst-case compliance. The only diagonal configurations present in the Pareto front for all branch lengths are $d=2$ and $d=9$ (underlined)

TZ branch length n	Pareto-optimal diagonal configurations d
2	<u>2</u> , <u>2</u> , 13, 15
3	6, <u>2</u> , <u>9</u> , 7, 10, 15, 13
4	<u>2</u> , <u>9</u> , 8, 13
5	<u>2</u> , <u>9</u> , 0
6	<u>2</u> , 10, 15, 11, <u>9</u>
7	<u>2</u> , 10, 8, 11, <u>9</u>

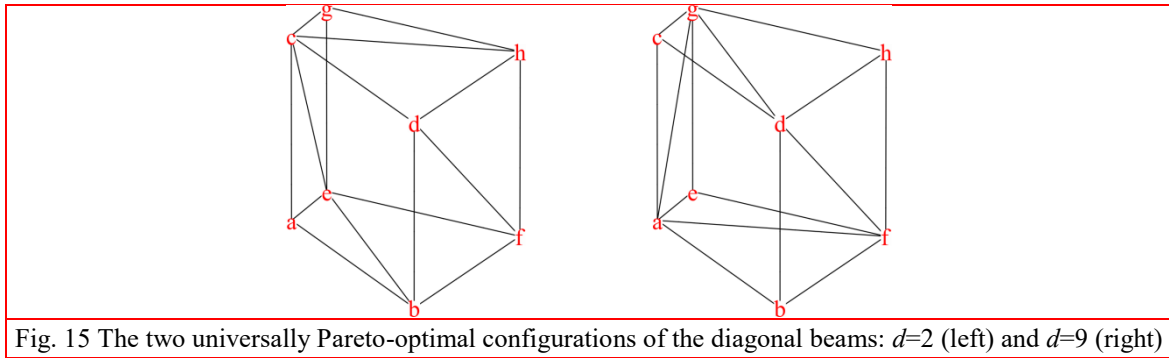


Fig. 15 The two universally Pareto-optimal configurations of the diagonal beams: $d=2$ (left) and $d=9$ (right)

4.2 Diameters of the beams

Fig. 16 shows the optimized diameters of the beams \bar{x} for the two universally Pareto-optimal configurations of the diagonals $d = 2$ and $d = 2$, as computed for all considered branch lengths $n = 2, 3, \dots, 7$. The corresponding maximum von Mises equivalent stresses of the beams are shown in Fig. 17; in accordance with Eq. (5), they are all below the assumed constraint of 100 MPa. It can be noticed that the stresses are very close to the constraint (the small variabilities seem to be numerical artifacts related to the inexact character of numerical optimization), and they fall considerably below it only if the diameter constraint Eq. (6) becomes active. Such a situation resembles the classical fully stressed designs of trusses (Razani 1965, Patnaik and Hopkins 1998), although it occurs here for ensembles S_n of frame structures and equivalent stresses.

A large difference can be noticed between the optimized diameters of the side beams (beams No. 2, 4, 6, 8, 9, 10, 11, 12, 14 and 15, see Fig. 4) and of the transverse beams of the floor and ceiling that join both TZ sides (beams No. 1, 3, 5, 7, 13 and 16). The difference can be intuitively explained by the fact that the sides of the TZ branch bear the global TZ load and transfer it to the global supports, while the transverse floor and ceiling beams transfer mostly only the local module load to the TZ sides. In the optimized structure, the side beams are thus much stiffer than the

transverse beams. An example TZ ramp is shown in Fig. 18. Each beam is drawn using its scaled optimized diameter. The configuration of modules is RLL_2R_2 , and the color convention is as in Fig. 2.

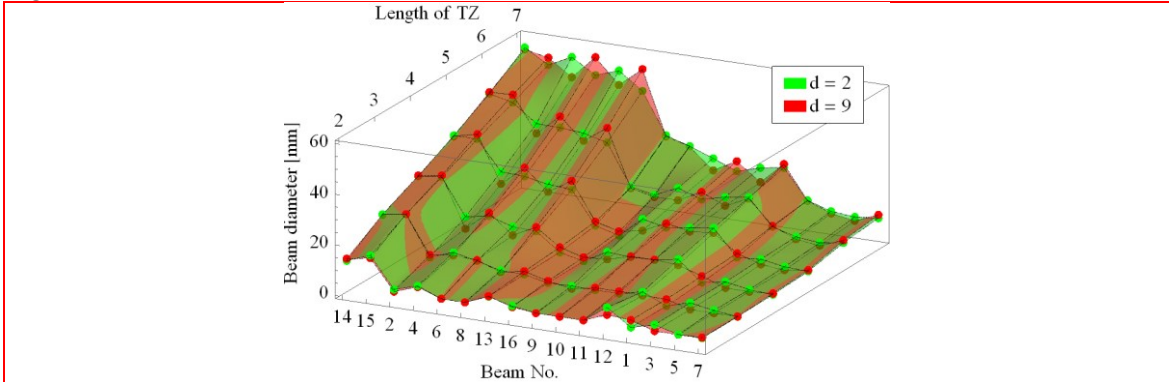


Fig. 16 The optimized values \bar{x} of the beam diameters obtained for the two universal Pareto-optimal configurations of the diagonals $d=2$ (green) and $d=9$ (red). The beam numbers have been re-ordered for clarity

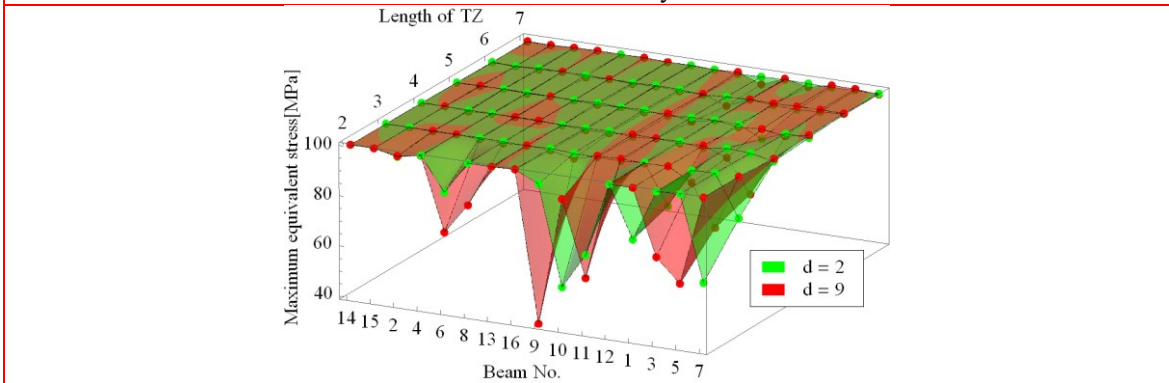


Fig. 17 The maximum von Mises equivalent stresses of the beams, computed for the optimized beam diameters shown in Fig. 16. The order of beams is the same as in Fig. 16

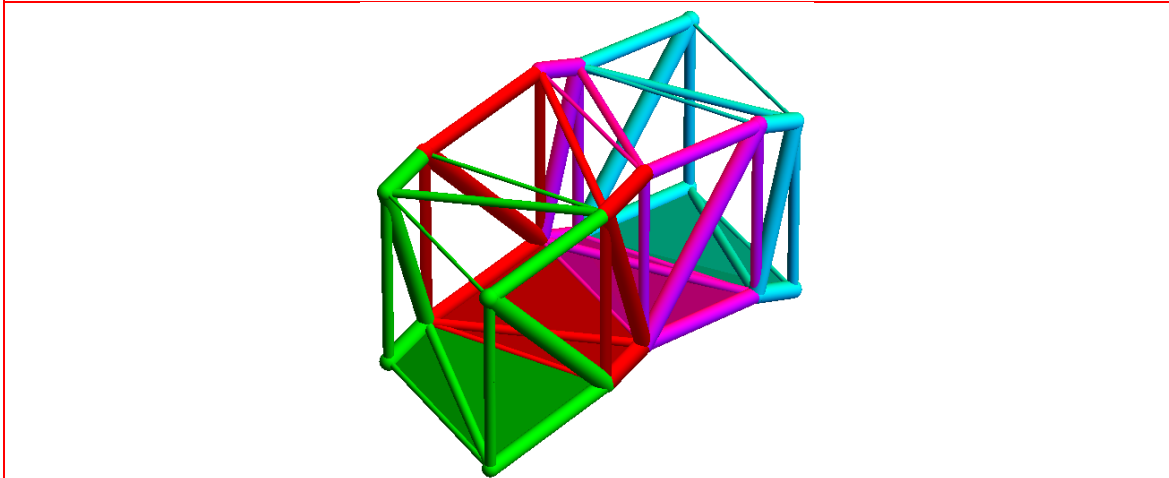


Fig. 18 An example TZ. The configuration of modules is RLL_2R_2 , and the color convention is as in Fig. 2. Each beam is drawn using its scaled optimized diameter

The maximum equivalent stresses shown in Fig. 17 might occur for various beams in a different module of the same n -module TZ branch or even in a different configuration s of the TZ branch. Fig. 19 shows these 16 worst-case configurations of 7-module TZs, as computed for the universally Pareto-optimal configuration $d = 2$ of the diagonals. Successive subplots correspond to the successive beams at the stress constraint. The most stressed beam is marked red and its number is explicitly printed in each subplot, for beam numbering see Fig. 4. The number in brackets denotes the number of the module with the most stressed beam, where the first unit is marked yellow, and the last unit is marked blue.

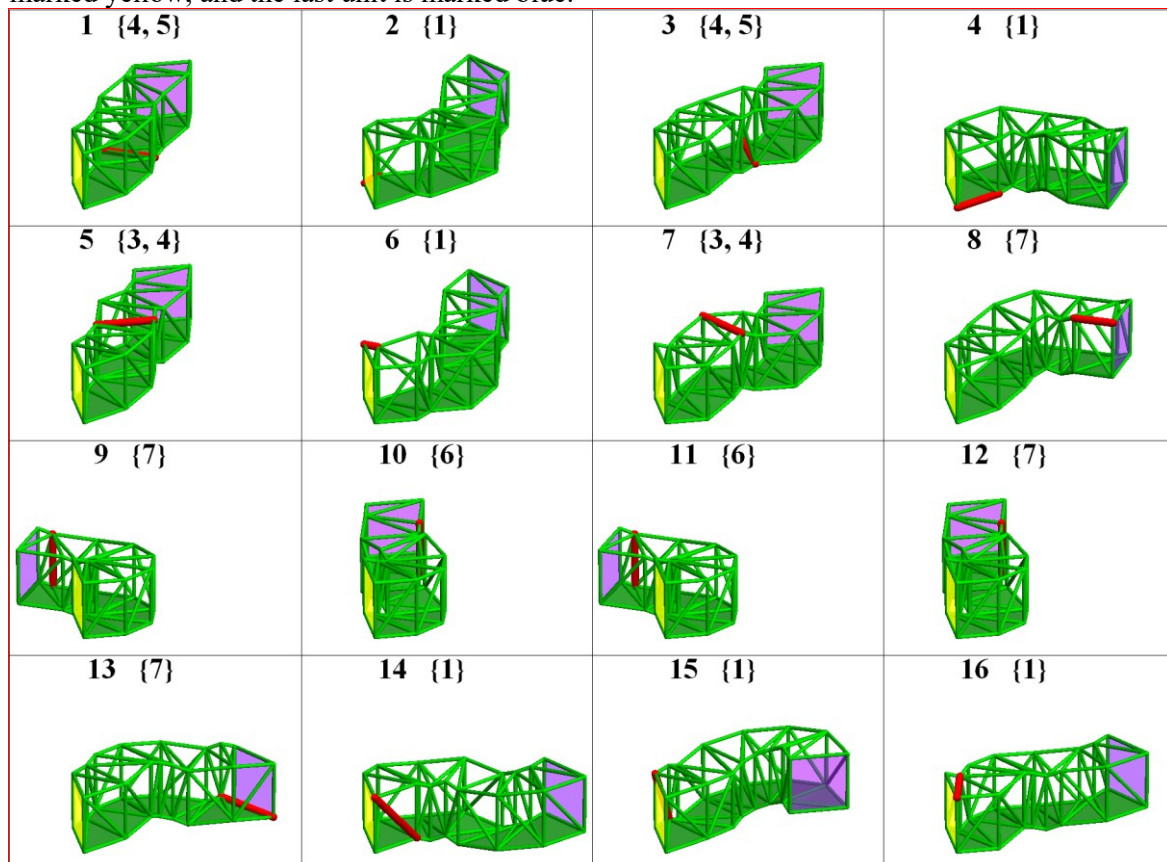


Fig. 19 The 16 worst-case TZ configurations s that correspond to the universally Pareto-optimum diagonal configuration $d=2$. The indices of the most stressed beams are shown on the top of each sub-figure, followed by the list of modules where such maximal stress occurs. In each case, the most stressed beam is highlighted in red

5. Conclusions

This paper presents the first attempt at structural optimization of single-branch Truss-Z modular structures. The outer geometry of the module is assumed to be defined by functional requirements and thus fixed. For optimization purposes, the structure is subjected to a distributed

static design load with the constrained equivalent von Mises stresses. The optimization variables are the diameters of the beams, as well as the internal topology of the module (configuration of its diagonals). The aim of optimization is to minimize the mass of the module. Besides the achieved minimum mass, the resulting designs are also assessed by their compliance under the design load, which is a typical aggregate measure of structural stiffness. With respect to other minimum mass problems, an important challenge is linked to the modularity of the system: the module must be designed for the worst-case scenario, as defined by the module position within a TZ branch and the geometric configuration of the branch itself. Therefore, instead of a typical single structure with a predefined single/multiple load condition, there are multiple structural configurations that need to be simultaneously assessed in order to optimize the worst-case performance.

In future work, modal characteristics and dynamic loads will be included in the optimization procedure. In particular, displacement and natural frequency constraints will be considered besides the stress constraints (Jalkanen and Koski 2005), and the problem of vibration damping will be studied (Lavan and Oded 2014, Poplawski *et al.* 2018). Moreover, geometric parameters of the module and the related criterion of TZ functionality will be included in a multicriterial type optimization (Martins and Lambe 2013).


Appendix

Table 3 outlines the optimization procedure described in Section 3.

Table 3 Outline of the optimization procedure

<p>For each considered set $S_n \in S$:</p> <ol style="list-style-type: none"> 1. Select the initial vector $\bar{\mathbf{x}}$ of the beam diameters. 2. For each configuration d of the diagonals: <ol style="list-style-type: none"> a. Compute the mass $m(\mathbf{x}, d)$ of the module. b. Compute the local stiffness matrix and the local load vector of a single module. c. For each configuration $s \in S_n$ <ol style="list-style-type: none"> i. Aggregate the local stiffness matrix and the local load vector of single modules into the global stiffness matrix and the global load vector of the configuration s. ii. Compute the global displacement vector and the compliance $C(\mathbf{x}, d, s)$. iii. For each beam, compute the local nodal reaction forces and use the circular hollow section formulas to compute the distribution of the von Mises stress and its maximum value. Store the maximum values, as found for each beam of the module, in the vector $\sigma^{\text{eq}}(\mathbf{x}, d, s)$. d. Take the maximum of $C(\mathbf{x}, d, s)$ w.r.t. all $s \in S_n$ to find the maximum (worst-case) compliance $C(\mathbf{x}, d, S_n)$. e. Take the maximum of the successive elements of $\sigma^{\text{eq}}(\mathbf{x}, d, s)$ w.r.t. all $s \in S_n$ to find the vector $\sigma^{\text{eq}}(\mathbf{x}, d, S_n)$ of the maximum von Mises stresses of the beams. f. Check the stress constraints. If not satisfied, update $\bar{\mathbf{x}}$ and go to Point 2a. g. Check the stop conditions. If not satisfied, update $\bar{\mathbf{x}}$ and go to Point 2a. h. Store the optimum $\bar{\mathbf{x}}(d, S_n)$, the corresponding mass of the module $m(d, S_n)$, the worst-case compliance $\bar{C}(d, S_n)$ and the maximum von Mises stresses of the beams $\sigma^{\text{eq}}(\bar{\mathbf{x}}, d, S_n)$.
--

Acknowledgments

This work was completed as part of the project titled: “*Extremely Modular Systems for temporary and permanent deployable structures and habitats: development, modeling, evaluation & optimization*”. It was funded by “*Polonez 2*” research grant no. 2016/21/P/ST8/03856 supported by the National Science Centre, Poland. This project has received funding from the European Union’s Horizon 2020 research and innovation programme under the Marie Skłodowska–Curie grant agreement No 665778 .

References

- Calafiore, G.C. and Dabene, F. (2008), “Optimization under uncertainty with applications to design of truss structures”, *Structural and Multidisciplinary Optimization*, **35**, 189-200.
- Christensen, P.W. and Klarbring, A. (2008), *An Introduction to Structural Optimization*, Springer Science & Business Media.
- Dunbar, G., Holland, C.A. and Maylor, E.A. (2004), “*Older Pedestrians: A Critical Review of the Literature*”, Road Safety Research Report No. 37, Department for Transport, London, England.
- Jalkanen, J. and Koski, J. (2005), “Heuristic methods in space frame optimization”, *Proceedings of the 46th AIAA/ASME/ASCE/AHS/ASC Structures, Structural Dynamics and Materials Conference*, Austin, Texas, USA.
- Lavan, O. and Oded, A. (2014), “Simultaneous topology and sizing optimization of viscous dampers in seismic retrofitting of 3D irregular frame structures”, *Earthquake Engineering & Structural Dynamics*, **43**(9), 1325-1342.
- Martins, J.R.R.A. and Lambe, A.B. (2013), “Multidisciplinary design optimization: A survey of architectures”, *AIAA Journal*, **51**(9), 2049-2075.
- Patnaik, S.N. and Hopkins, D.A. (1998), “Optimality of a fully stressed design”, *Computer Methods in Applied Mechanics and Engineering*, **165**(1-4), 215-221.
- Pollack, M.E. (2005), “Intelligent technology for an aging population: The use of AI to assist elders with cognitive impairment”, *Artificial Intelligence Magazine*, **26**(2), 9-24.
- Poplawski, B., Mikułowski, G., Mróz, A. and Jankowski, Ł. (2018), “Decentralized semi-active damping of free structural vibrations by means of structural nodes with an on/off ability to transmit moments”, *Mechanical Systems and Signal Processing*, **100**, 926-939.
- Razani, A. (1965), “Behavior of fully stressed design of structures and its relationship to minimum-weight design”, *AIAA Journal*, **3**(12), 2262-2268.
- Torstenfelt, B. and Klarbring, A. (2006), “Structural optimization of modular product families with application to car space frame structures”, *Structural and Multidisciplinary Optimization*, **32**(2), 133-140.
- Tugilimana, A., Thrall, A.P. and Coelho, R.F. (2017), “Conceptual design of modular bridges including layout optimization and component reusability”, *Journal of Bridge Engineering*, **22**(11), 04017094.
- Zawidzki, M. and Tateyama, K. (2011), “Application of evolution strategy for minimization of the number of modules in a truss branch created with the Truss-Z system”, *Proceedings of the 2nd International Conference on Soft Computing Technology in Civil, Structural and Environmental Engineering*, Civil-Comp Press, Stirlingshire, UK, Paper 9.
- Zawidzki, M. (2011), *Tiling of a Path with Trapezoids in a Constrained Environment with Backtracking Algorithm*, Wolfram Demonstrations Project, <http://demonstrations.wolfram.com/TilingOfAPathWithTrapezoidsInAConstrainedEnvironmentWithBack>
- Zawidzki, M. and Nishinari, K. (2012), “Modular Truss-Z system for self-supporting skeletal free-form pedestrian networks”, *Advances in Engineering Software*, **47**(1), 147-159.

- Zawidzki, M. and Nishinari, K. (2013), "Application of evolutionary algorithms for optimum layout of Truss-Z linkage in an environment with obstacles", *Advances in Engineering Software*, **65**, 43-59.
- Zawidzki, M. (2013), "Creating organic 3-dimensional structures for pedestrian traffic with reconfigurable modular Truss-Z system", *International Journal of Design & Nature and Ecodynamics*, **8**(1), 61-87.
- Zawidzki, M. (2015), "Retrofitting of pedestrian overpass by Truss-Z modular systems using graph-theory approach", *Advances in Engineering Software*, **81**, 41-49.